




Neural echo state network using oscillations of gas bubbles in water

Ivan S. Maksymov *

Optical Sciences Centre, Swinburne University of Technology, Hawthorn, Victoria 3122, Australia

Andrey Pototsky  and Sergey A. Suslov 

Department of Mathematics, Swinburne University of Technology, Hawthorn, Victoria 3122, Australia



(Received 23 December 2021; accepted 21 March 2022; published 13 April 2022)

In the framework of physical reservoir computing (RC), machine learning algorithms designed for digital computers are executed using analog computerlike nonlinear physical systems that can provide energy-efficient computational power for predicting time-dependent quantities that can be found using nonlinear differential equations. We suggest a bubble-based RC (BRC) system that combines the nonlinearity of an acoustic response of a cluster of oscillating gas bubbles in water with a standard echo state network (ESN) algorithm that is well suited to forecast chaotic time series. We confirm the plausibility of the BRC system by numerically demonstrating its ability to forecast certain chaotic time series similarly to or even more accurately than ESN.

DOI: [10.1103/PhysRevE.105.044206](https://doi.org/10.1103/PhysRevE.105.044206)

I. INTRODUCTION

Forecasting the time evolution of dynamical systems is important for understanding many natural phenomena such as the behavior of living organisms and the variation of the Earth's climate, for predicting stock markets, and for controlling autonomous vehicles [1]. However, the nonlinearity of such systems considerably complicates the task of prediction, which forces the modern machine learning (ML) algorithms to rely on longer observation times. Substantial computational resources are needed to process such big data sets.

Reservoir computing (RC) [2–5] and its foundation concepts of echo state networks (ESNs) [2,6] and liquid state machines (LSMs) [7,8] underpin an emergent approach to ML that is especially well suited for forecasting the response of nonlinear dynamical systems that exhibit chaotic or complex spatiotemporal behavior [4,6,9–11], the problem that is difficult to resolve using traditional ML algorithms [12]. In an RC system [Fig. 1(a)], an artificial neural network is structured as a combination of a fast output layer and a much slower body of the network called the reservoir [13]. Such an arrangement helps to resolve especially challenging forecasting problems, including free-running generation of time series, where a trained RC system is presented with previously unseen data and is tasked with making a forecast using its own output from the previous time steps [4,14,15].

The standard ESN algorithm laying a foundation of RC uses the following nonlinear update equation [2,6,14]:

$$\vec{x}_n = (1 - \alpha)\vec{x}_{n-1} + \alpha \tanh(\mathbf{W}^{\text{in}}\vec{u}_n + \mathbf{W}\vec{x}_{n-1}), \quad (1)$$

where n is the index denoting entries corresponding to equally spaced discrete time instances t_n , \vec{u}_n is the vector of N_u input values, \vec{x}_n is a vector of N_x neural activations of the reservoir,

the operator $\tanh(\cdot)$ applied elementwise to its arguments is a typical sigmoid activation function used in the nonlinear model of a neuron [16], \mathbf{W}^{in} is the input matrix consisting of $N_x \times N_u$ elements, \mathbf{W} is the recurrent weight matrix containing $N_x \times N_x$ elements, and $\alpha \in (0, 1]$ is the leaking rate that controls the update speed of the reservoir's temporal dynamics.

To train the linear readout of ESN, one calculates the output weights \mathbf{W}^{out} by solving a system of linear equations, $\mathbf{Y}^{\text{target}} = \mathbf{W}^{\text{out}}\mathbf{X}$, where the state matrix \mathbf{X} and the target matrix $\mathbf{Y}^{\text{target}}$ are constructed using, respectively, \vec{x}_n and the vector of target outputs $\vec{y}_n^{\text{target}}$ as columns for each time instant t_n . The solution is often obtained in the form $\mathbf{W}^{\text{out}} = \mathbf{Y}^{\text{target}}\mathbf{X}^T(\mathbf{X}\mathbf{X}^T + \beta\mathbf{I})^{-1}$, where \mathbf{I} is the identity matrix, $\beta = 10^{-8}$ is a regularization coefficient, and \mathbf{X}^T is the transpose of \mathbf{X} [14]. Then, one uses the trained ESN, solves Eq. (1) for new input data \vec{u}_n , and computes the output vector $\vec{y}_n = \mathbf{W}^{\text{out}}\vec{x}_n$ (in our case, a more common form $\vec{y}_n = \mathbf{W}^{\text{out}}[1; \vec{u}_n; \vec{x}_n]$ optimized to forecast complex nonlinear time series using a constant bias and the concatenation $[\vec{u}_n; \vec{x}_n]$ [2,14], produced qualitatively similar results). We note that ESN needs to know the target data only when it is trained since for forecasting it uses its own output from the previous time step, i.e., \vec{x}_n is calculated using Eq. (1) with $\vec{u}_n = \vec{y}_{n-1}$. However, the target data may still be needed to assess the accuracy of the forecast made by ESN.

The performance tests of ESN are conducted using target chaotic Mackey-Glass time series (MGTS) [14] that are produced by the delay differential equation [17]

$$\dot{x}_{\text{MG}}(t) = \beta_{\text{MG}} \frac{x_{\text{MG}}(\tau_{\text{MG}} - t)}{1 + x_{\text{MG}}^q(\tau_{\text{MG}} - t)} - \gamma_{\text{MG}} x_{\text{MG}}(t), \quad (2)$$

where one typically chooses $\tau_{\text{MG}} = 17$ and sets $q = 10$, $\beta_{\text{MG}} = 0.2$, and $\gamma_{\text{MG}} = 0.1$ [14]. MGTS with these parameters is uniquely suited for a demonstration of the abilities of ESN to forecast chaotic time series [18].

*imaksymov@swin.edu.au

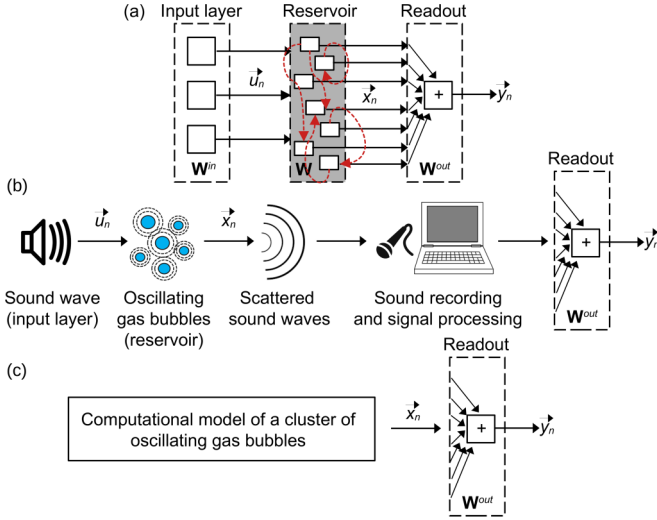


FIG. 1. (a) ESN algorithm. The reservoir is a network of interconnected dynamical components (shown by dashed arrows); only the linear readout is trained to produce the output. (b) The approach proposed in this work. Complex interactions between the oscillating gas bubbles in water play the role of a reservoir, but the readout is trained using the ESN algorithm. (c) Schematic of simulations used to demonstrate the plausibility of the BRC system.

However, ESN is essentially a program for a digital computer and its ability to forecast is limited by the available computational resources. Therefore, it has been suggested that the ESN algorithm can be implemented using certain nondigital nonlinear physical systems [5,19,20], which at the conceptual model level means that Eq. (1) is replaced with the respective nonlinear differential equation describing the dynamics of a particular physical system. Similarly to analog computers that can solve certain problems more efficiently than their digital counterparts [21–24], physical RC systems may provide energy efficiency in practical situations, where the relationship between time-dependent physical quantities that needs to be predicted can be expressed using solutions of nonlinear differential equations. A number of physical RC networks have been demonstrated using spintronic systems [25–27], liquids [28,29], quantum ensembles [30], and electronic [5], photonic [5,31], and mechanical devices [5,32].

II. GAS BUBBLE-BASED RC SYSTEM

Here, we propose [Fig. 1(b)] and computationally validate [Fig. 1(c)] an approach to RC, where the nonlinear dynamics of a reservoir is represented by weakly nonlinear oscillations of a cluster of gas bubbles in water driven by an acoustic pressure wave [33]. Previously, we demonstrated that in a cluster of mm-sized bubbles with randomly chosen equilibrium radii and initial spatial positions, each bubble emits a unique acoustic signal that reflects a complex nature of its interaction with the neighboring bubbles [34]. Furthermore, we suggested an acoustic frequency comb technique that can be used to reliably detect such signals [34,35]. Thus, a cluster consisting of N_b randomly sized and positioned bubbles can be used as a reservoir network of $N_b \times N_b$ random connections,

where the acoustic response of individual bubbles can serve as a physical counterpart of the neural activation states of ESN [2,6].

We replace Eq. (1) by the Rayleigh-Plesset equation of nonlinear dynamics of spherical gas bubble oscillations [33,34] in a cluster consisting of N_b bubbles not undergoing translational motion [33,34],

$$R_p \ddot{R}_p + \frac{3}{2} \dot{R}_p^2 = \frac{1}{\rho} [P_p - P_\infty(t)] - P_{sp}, \quad (3)$$

where overdots denote differentiation with respect to time and, for the p th bubble in the cluster,

$$P_p = \left(P_0 - P_v + \frac{2\sigma}{R_{p0}} \right) \left(\frac{R_{p0}}{R_p} \right)^{3\kappa} - \frac{4\mu}{R_p} \dot{R}_p - \frac{2\sigma}{R_p}. \quad (4)$$

The term accounting for the pressure acting on of the p th bubble due to scattering of the incoming pressure wave by the neighboring bubbles in a cluster is given by

$$P_{sp} = \sum_{l=1, l \neq p}^{N_b} \frac{1}{d_{pl}} (R_l^2 \ddot{R}_l + 2R_l \dot{R}_l^2), \quad (5)$$

where d_{pl} is the interbubble distance and parameters R_{p0} and $R_p(t)$ are the equilibrium and instantaneous radii of the p th bubble in the cluster. The term $P_\infty(t) = P_0 - P_v + \alpha_s u_s(t)$ represents the time-dependent pressure in the liquid far from the bubble, where α_s and $u_s(t)$ are the amplitude and temporal profile of the sound wave driving oscillations of the bubbles. The acoustic power scattered by the p th bubble in the cluster in the far-field zone at the distance h is [34]

$$P_{\text{scat}}(R_p, t) = \frac{\rho R_p}{h} (R_p \ddot{R}_p + 2\dot{R}_p^2). \quad (6)$$

To incorporate Eq. (3) into the linear readout of ESN, we sample $P_{\text{scat}}(R_p, t)$ and $u_s(t)$ at equidistant time instances and obtain their discrete analogs that we treat as the vectors of neural activations \bar{x}_n and of input values \bar{u}_n of ESN, respectively. To train the bubble-based RC (BRC) system, we use MGTS $x_{\text{MG}}(t)$ obtained from Eq. (2) as the driving sound signal $u_s(t)$. However, when the BRC system makes a forecast, it does not know the target series because $u_s(t)$ is defined by the discrete network output \bar{y}_n .

III. RESULTS AND DISCUSSION

The signal amplitude $u_s(t)$ is chosen to be small ($\alpha_s = 0.1 - 1$ kPa, i.e., $\alpha_s \ll P_0$) so that both the nonlinearity of bubble oscillations and Bjerknes forces acting between bubbles in the cluster [33] remain weak. Such physical conditions allow a cluster of mm-sized bubbles to remain stable over a time sufficient to train and exploit the BRC system before the configuration of the cluster changes due to the translational motion of bubbles [34]. The cluster stability is important because the topology of a reservoir must not change during its training and use [14]. The operation of the BRC system in a weakly nonlinear regime also helps to satisfy the echo state condition that implies that dynamics of the neural activations \bar{x}_n is uniquely defined by a given input signal \bar{u}_n [6].

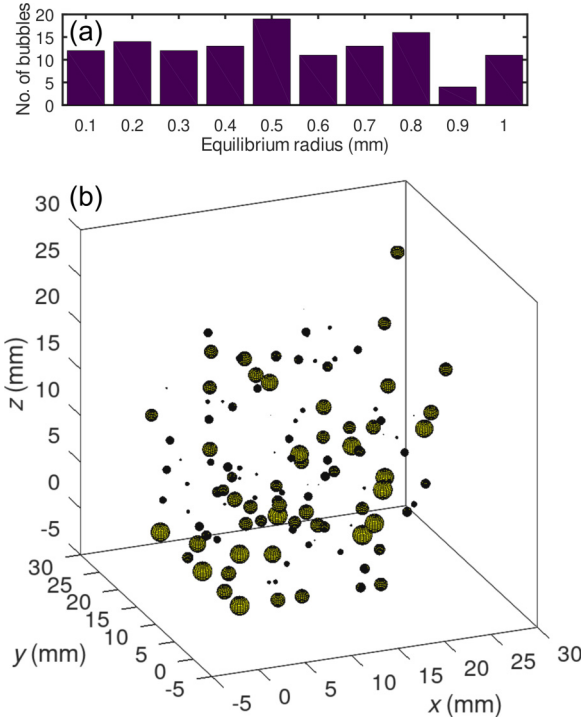


FIG. 2. (a) Size and (b) spatial distribution of bubbles in a representative cluster used as the physical reservoir.

Physically, this means that the phase space of Eq. (3) does not contain multiple periodic or chaotic attractors or fixed points.

For our simulations, we generate a cluster consisting of 125 bubbles with equilibrium radii randomly chosen in the 0.1 to 1 mm range (Fig. 2). We use the following model parameters corresponding to water at 20°C: $\mu = 10^{-3}$ kg m/s, $\sigma = 7.25 \times 10^{-2}$ N/m, $\rho = 10^3$ kg/m³, $P_v = 2330$ Pa, $P_0 = 10^5$ Pa, and $\kappa = 4/3$ [34]. Relevant computational details can also be found in [34].

The dynamics of a cluster of oscillating bubbles also has to match the speed of the temporal evolution of the training time series. In ESN, this is achieved using the leaking rate α in Eq. (1) [14]. In our BRC system, the dynamics of the network is controlled by ensuring that the frequency of the major peak f_{MG} in the Fourier spectrum of the time series $x_{MG}(t)$ is close to the frequency of natural oscillations of individual bubbles, with the most representative equilibrium radius in Fig. 2(a) (using the well-known Minnaert formula [33], we obtain $f_{MG} \approx 6.5$ kHz). To tune f_{MG} , it is convenient to change the timescale of previously tabulated $x_{MG}(t)$, for example, by using an auxiliary discrete time instant in a computer program that solves Eq. (3). Once the trained network has produced an output signal, the original timescale is restored.

The advantage of such a rescaling procedure is that a cluster of mm-sized bubbles can be used to forecast time series with disparate timescales. Indeed, the dynamics of the BRC system could also be accelerated by decreasing the equilibrium radius of bubbles (and thus increasing their natural frequency). However, the generation of microscopic bubbles requires special techniques [36]. In addition, microscopic bubbles are effectively stiffer than mm-sized ones [33] so that measurements involving them require special high-frequency

and high-power ultrasonic equipment compared with a technically simple acoustic setup sufficient for studying mm-sized bubbles [35].

In Fig. 3(a), we demonstrate the ability of a trained BRC system to forecast MGTS. We also compare the accuracy of its forecast with that of ESN with $N_x = 125$, which is equivalent to the size of the BRC reservoir. In the time interval 0–1 ms, the BRC system correctly reproduces both the pattern and the timeline of MGTS. The mean-square error (MSE)—a standard measure of the accuracy of ESNs [14]—is approximately 5×10^{-2} for the BRC system, which is two orders of magnitude larger than that for ESN, thereby indicating that in a short-term perspective, ESN performs better. However, over the full test interval 0–2 ms, the MSE of both RC systems is approximately 0.5×10^{-2} , which indicates that the long-term behavior of the BRC system may be closer to the target than that of ESN.

Nevertheless, the observed behavior of ESN is widely regarded as a positive outcome for chaotic systems with limited availability of information [2,4,6]. Indeed, many other competitive neural network architectures either fail to deliver similar results using small data sets or can produce acceptable results only using much bigger data sets (and therefore requiring substantial computational resources) [2,12,13]. These features make ESN the best-in-class ML algorithm designed to forecast highly nonlinear and chaotic time series [4]. Given this, the ability of a much simpler BRC system to predict MGTS similarly to, and in some aspects matching the target better than ESN is a significant result. While without any optimization attempted so far the accuracy of the BRC system may not be as high as that of ESN in a short term, it can be advantageously used in applications tolerating a lower accuracy of the forecast [37] or if a long-term reliability of a forecast is the priority.

Results quantitatively similar to those in Fig. 3(a) were obtained for other clusters that were randomly generated using the same set of equilibrium bubble radii. Significantly, all forecast time series had a phase lag with respect to the target signal. The existence of a phase shift between the driving sound pressure and acoustic power scattered by a single gas bubble is a well-established fact [33]. This effect is also present in the bubble-cluster reservoir, where bubble oscillations are driven by a continuous acoustic signal produced using the discrete output of the network. The phase lag was essentially the same for all random cluster configuration of similarly sized bubbles. This is because the bubble response delay is caused by the inertia of liquid surrounding them that depends only on their sizes. Subsequently, this phase lag was removed from all relevant results during postprocessing.

To forecast time series that exhibit a more chaotic behavior than MGTS, ESNs require a larger reservoir and a delicate case-by-case tuning of its algorithmic parameters [14]. On the other hand, the BRC system could solve specific classes of problems more efficiently than ESN without the need to modify the configuration of the gas bubble cluster. In particular, similarly to certain analog computational systems [21,38], the use of our BRC system could help avoid limitations imposed by time-step discretization needed to numerically solve differential equations arising in practice [22–24].

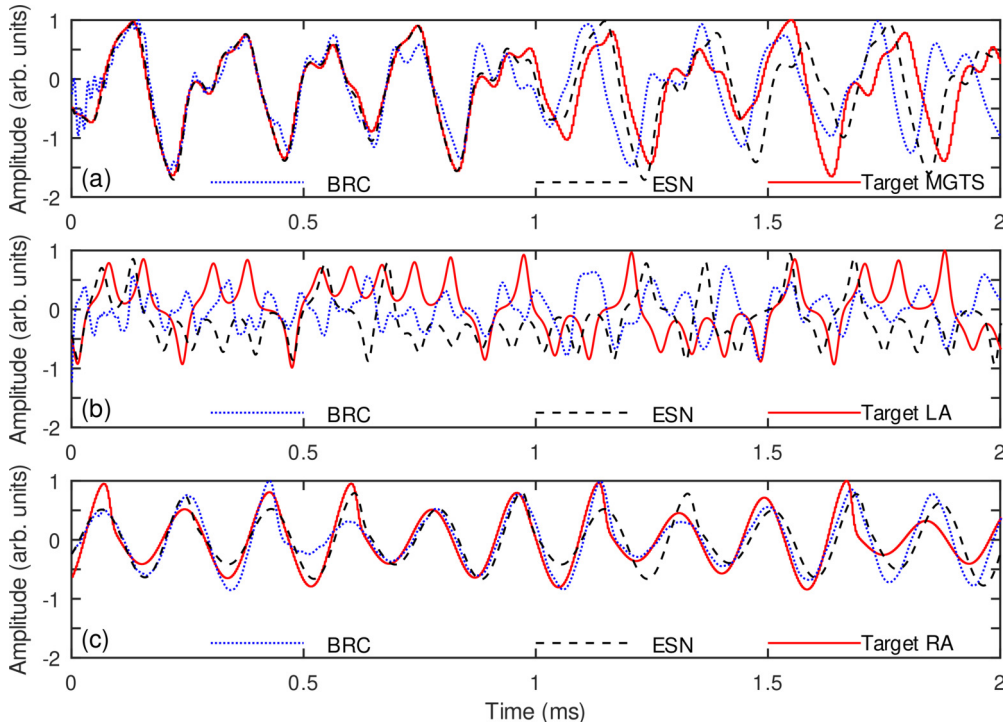


FIG. 3. The BRC (dotted lines) and ESN (dashed lines) forecasts compared with the target (a) MGTS, (b) LA, and (c) RA (solid lines). The target data, which are plotted here for reference only, are not used by the RC systems. In ESN, the leaking rate α equals 0.3, 0.1, and 0.01 for MGTS, LA, and RA, respectively.

To verify this assertion, we compare the performance and implementation cost of ESN and the BRC system to forecast the behavior of Lorenz (LA) [39] and Rössler (RA) [40] attractors. We keep the same parameters for both RC systems as in the tests with MGTS, but allow variations of the leaking rate α of ESN. The implementation details and discussion of the system performance can be found in the Supplemental Material [41]. As seen in Fig. 3(b), neither the BRC system nor ESN can follow the long-term behavior of LA. ESN may be able to mimic the behavior of LA somewhat better initially, but overall it suffers from an apparent negative bias underpredicting the LA output over most of the test interval. In contrast, the BRC system produces values that are, on average, much closer to the target, but it misses some of fine details of the LA behavior. Indeed, in the time interval 0–2 ms, the BRC system has $\text{MSE} = 0.33$ compared with 0.55 for ESN, which speaks in favor of the BRC system. At the same time, the BRC system has a clear advantage in terms of the implementation cost. For example, to obtain the ESN prediction of LA presented in Fig. 3(b), a lengthy procedure of tuning the value of the leaking rate α had to be followed to avoid numerical instabilities caused by artifacts of the time-step discretization of Eq. (1) and by the fact that the size of the chosen reservoir had to be kept small to enable a meaningful comparison (in general, to produce a qualitatively accurate output, ESN requires a reservoir with a much larger size than that used here).

Whereas significant tuning was also needed to enable ESN to forecast RA, the BRC system could forecast RA without any optimization [Fig. 3(c)]. Significantly, MSE of the BRC

system for the interval 0–2 ms is approximately 0.06 compared with 0.31 for ESN. This result strongly speaks in favor of the proposition that the BRC system could outperform ESN in some practical situations. We established that the BRC system can predict RA because, similarly to MGTS, the Fourier spectrum of RA has well-defined frequency peaks (see the Supplemental Material [41]). As a result, the oscillating bubbles of the BRC reservoir can match the frequencies of the peaks. In contrast, the spectrum of LA is continuous and has no well-defined discrete peaks. This is the reason why the BRC system inherently possessing a discrete spectrum cannot accurately forecast LA or any other continuous-spectrum signal. Several potential approaches to resolving this challenge are discussed in the Supplemental Material [41].

IV. CONCLUSIONS

In conclusion, we have demonstrated through numerical simulations that an RC system employing a cluster of oscillating gas bubbles in water as the reservoir can forecast certain chaotic time series similarly to ESN. Although the currently achievable accuracy of the proposed RC system may be lower than that of highly optimized ESN, it can be increased using, for example, novel techniques of gas bubble-cluster manipulation [34,35]. In certain practically important cases (e.g., when the spectrum of the target signal has well-defined peaks), the size of the BRC reservoir required to achieve comparable accuracy may be significantly smaller than that of ESN, and it may require no or little tuning compared to that needed for ESN. Moreover, since its prototype can be

built using energy-efficient integrated electronic circuits and piezoelectric transducers, BRC holds the promise of being less expensive to build and, at the same time, more computationally and energy efficient to run than an ESN implemented on a workstation computer.

ACKNOWLEDGMENTS

I.S.M. acknowledges the support from the Australian Research Council via the Future Fellowship (Grant No. FT180100343) program and useful discussions with Prof. Mikhail Kostylev (The University of Western Australia).

-
- [1] M. Small, *Applied Nonlinear Time Series Analysis: Applications in Physics, Physiology and Finance* (World Scientific, Singapore, 2005).
- [2] M. Lukoševičius and H. Jaeger, Reservoir computing approaches to recurrent neural network training, *Comput. Sci. Rev.* **3**, 127 (2009).
- [3] D. Verstraeten, B. Schrauwen, M. D’Haene, and D. Stroobandt, An experimental unification of reservoir computing methods, *Neural Netw.* **20**, 391 (2007).
- [4] D. J. Gauthier, E. Bollt, A. Griffith, and W. A. S. Barbosa, Next generation reservoir computing, *Nat. Commun.* **12**, 5564 (2021).
- [5] K. Nakajima and I. Fisher, *Reservoir Computing* (Springer, Berlin, 2021).
- [6] H. Jaeger, *A tutorial on training recurrent neural networks, covering BPPT, RTRL, EKF and the echo state network approach*, GMD Report No. 159 (German National Research Center for Information Technology, Sankt Augustin, Germany, 2005).
- [7] W. Maass, T. Natschläger, and H. Markram, Real-time computing without stable states: A new framework for neural computation based on perturbations, *Neural Comput.* **14**, 2531 (2002).
- [8] W. Maass and H. Markram, On the computational power of recurrent circuits of spiking neurons, *J. Comput. Syst. Sci.* **69**, 593 (2004).
- [9] J. Pathak, Z. Lu, B. R. Hunt, M. Girvan, and E. Ott, Using machine learning to replicate chaotic attractors and calculate Lyapunov exponents from data, *Chaos* **27**, 121102 (2017).
- [10] J. Pathak, B. Hunt, M. Girvan, Z. Lu, and E. Ott, Model-Free Prediction of Large Spatiotemporally Chaotic Systems from Data: A Reservoir Computing Approach, *Phys. Rev. Lett.* **120**, 024102 (2018).
- [11] A. Chattopadhyay, P. Hassanzadeh, and D. Subramanian, Data-driven predictions of a multiscale Lorenz 96 chaotic system using machine-learning methods: Reservoir computing, artificial neural network, and long short-term memory network, *Nonlin. Proc. Geophys.* **27**, 373 (2020).
- [12] P. Chen, R. Liu, K. Aihara, and L. Chen, Autoreservoir computing for multistep ahead prediction based on the spatiotemporal information transformation, *Nat. Commun.* **11**, 4568 (2020).
- [13] U. D. Schiller and J. J. Steil, Analyzing the weight dynamics of recurrent learning algorithms, *Neurocomputing* **63**, 5 (2005).
- [14] M. Lukoševičius, A practical guide to applying echo state networks, in *Neural Networks: Tricks of the Trade, Reloaded*, edited by G. Montavon, G. B. Orr, and K.-R. Müller (Springer, Berlin, 2012), pp. 659–686.
- [15] M. Lukoševičius and A. Uselis, Efficient implementations of echo state network crossvalidation, *Cogn. Comput.* (2021), doi: 10.1007/s12559-021-09849-2.
- [16] S. Haykin, *Neural Networks: A Comprehensive Foundation* (Pearson-Prentice Hall, Singapore, 1998).
- [17] M. C. Mackey and L. Glass, Oscillation and chaos in physiological control systems, *Science* **197**, 287 (1977).
- [18] H. Jaeger and H. Haas, Harnessing nonlinearity: Predicting chaotic systems and saving energy in wireless communication, *Science* **304**, 78 (2004).
- [19] G. Tanaka, T. Yamane, J. B. Héroux, R. Nakane, N. Kanazawa, S. Takeda, H. Numata, D. Nakano, and A. Hirose, Recent advances in physical reservoir computing: A review, *Neural Newt.* **115**, 100 (2019).
- [20] K. Nakajima, Physical reservoir computing—An introductory perspective, *Jpn. J. Appl. Phys.* **59**, 060501 (2020).
- [21] D. E. Hyndman, *Analog and Hybrid Computing* (Pergamon, Oxford, 1970).
- [22] G. E. R. Cowan, R. C. Melville, and Y. P. Tsividis, A VLSI analog computer/digital computer accelerator, *IEEE J. Solid-State Circuits* **41**, 42 (2006).
- [23] M. C. Soriano, S. Ortín, L. Keuninckx, L. Appeltant, J. Danckaert, L. Pesquera, and G. van der Sande, Delay-based reservoir computing: Noise effects in a combined analog and digital implementation, *IEEE Trans. Neural Netw. Learn. Syst.* **26**, 388 (2015).
- [24] F. Zangeneh-Nejad and R. Fleury, Performing mathematical operations using high-index acoustic metamaterials, *New J. Phys.* **20**, 073001 (2018).
- [25] T. Furuta, K. Fujii, K. Nakajima, S. Tsunegi, H. Kubota, Y. Suzuki, and S. Miwa, Macromagnetic Simulation for Reservoir Computing Utilizing Spin Dynamics in Magnetic Tunnel Junctions, *Phys. Rev. Appl.* **10**, 034063 (2018).
- [26] M. Riou, J. Torrejon, B. Garitainé, F. A. Araujo, P. Bortolotti, V. Cros, S. Tsunegi, K. Yakushiji, A. Fukushima, H. Kubota, S. Yuasa, D. Querlioz, M. D. Stiles, and J. Grollier, Temporal Pattern Recognition with Delayed-Feedback Spin-Torque Nano-Oscillators, *Phys. Rev. Appl.* **12**, 024049 (2019).
- [27] S. Watt and M. Kostylev, Reservoir Computing Using a Spin-Wave Delay-Line Active-Ring Resonator Based on Yttrium-Iron-Garnet Film, *Phys. Rev. Appl.* **13**, 034057 (2020).
- [28] C. Fernando and S. Sojakka, Pattern recognition in a bucket, in *Advances in Artificial Life*, edited by W. Banzhaf, J. Ziegler, T. Christaller, P. Dittrich, and J. T. Kim (Springer, Berlin, 2003), pp. 588–597.
- [29] K. Nakajima and T. Aoyagi, The memory capacity of a physical liquid state machine, *IEICE Tech. Rep.* **115**, 109 (2015).
- [30] K. Fujii and K. Nakajima, Harnessing Disordered-Ensemble Quantum Dynamics for Machine Learning, *Phys. Rev. Appl.* **8**, 024030 (2017).
- [31] M. Sorokina, S. Sergeev, and S. Turitsyn, Fiber echo state network analogue for high-bandwidth dual-quadrature signal processing, *Opt. Express* **27**, 2387 (2019).
- [32] J. C. Coulombe, M. C. A. York, and J. Sylvestre, Computing with networks of nonlinear mechanical oscillators, *PLoS ONE* **12**, e0178663 (2017).

- [33] W. Lauterborn and T. Kurz, Physics of bubble oscillations, *Rep. Prog. Phys.* **73**, 106501 (2010).
- [34] B. Q. H. Nguyen, I. S. Maksymov, and S. A. Suslov, Spectrally wide acoustic frequency combs generated using oscillations of polydisperse gas bubble clusters in liquids, *Phys. Rev. E* **104**, 035104 (2021).
- [35] B. Q. H. Nguyen, I. S. Maksymov, and S. A. Suslov, Acoustic frequency combs using gas bubble cluster oscillations in liquids: A proof of concept, *Sci. Repts.* **11**, 38 (2021).
- [36] C. Chen, Y. Zhu, P. W. Leech, and R. Manasseh, Production of monodispersed micron-sized bubbles at high rates in a microfluidic device, *Appl. Phys. Lett.* **95**, 144101 (2009).
- [37] E. J. de Fortuny, T. D. Smedt, D. Martens, and W. Daelemans, Evaluating and understanding text-based stock price prediction models, *Inf. Proc. Manag.* **50**, 426 (2014).
- [38] J. van Veen, Analogy between tides and AC electricity, *The Engineer* **20**, 498 (1947).
- [39] E. N. Lorenz, Deterministic nonperiodic flow, *J. Atmos. Sci.* **20**, 130 (1963).
- [40] O. E. RöSSLer, An equation for continuous chaos, *Phys. Lett. A* **57**, 397 (1976).
- [41] See Supplemental Material at <http://link.aps.org/supplemental/10.1103/PhysRevE.105.044206> for additional information, which includes Refs. [42–47].
- [42] Y. A. Kosevich, Nonlinear Sinusoidal Waves and Their Superposition in Anharmonic Lattices, *Phys. Rev. Lett.* **71**, 2058 (1993).
- [43] K. Ikeda, Multiple-valued stationary state and its instability of the transmitted light by a ring cavity system, *Opt. Commun.* **30**, 257 (1979).
- [44] N. H. Packard, J. P. Crutchfield, J. D. Farmer, and R. S. Shaw, Geometry from a Time Series, *Phys. Rev. Lett.* **45**, 712 (1980).
- [45] M. Hénon, A two-dimensional mapping with a strange attractor, *Commun. Math. Phys.* **50**, 69 (1976).
- [46] J. C. Sprott, A simple chaotic delay differential equation, *Phys. Lett. A* **366**, 397 (2007).
- [47] Z. Li and G. Tanaka, Multi-reservoir echo state networks with sequence resampling for nonlinear time-series prediction, *Neurocomputing* **467**, 115 (2022).